A Seismological Portrait of the Anomalous 1996 Bardarbunga Volcano, Iceland, Earthquake

Hrvoje Tkalčić[1], Douglas S. Dreger[2], Gillian R. Foulger[3], Bruce R. Julian[4] and Andreas Fichtner[5]

[1]*Research School of Earth Sciences, Australian National University, Canberra ACT 0200, Australia;* [2]*Berkeley Seismological Laboratory, University of California at Berkeley, Berkeley, CA 94720, USA;*
[3]*Department of Earth Sciences, Durham University, Durham DH13LE, UK;* [4]*United States Geological Survey, Menlo Park, CA 94025, USA;*
[5]*Department of Earth Sciences, Utrecht University, 3508 TA Utrecht, Netherlands*

1. Summary

The Bardarbunga volcano lies beneath the 500-m-thick Vatnajokull icecap, the largest glacier in Europe. An earthquake with Mw 5.6 and a strong non-double-couple (NDC) radiation pattern occurred beneath the caldera on 29 September, 1996. A peculiarity of this earthquake was that it was the first in a sequence of seismic and magmatic events and that it was followed, not preceded or accompanied, by a major eruption which ultimately led to a breakout flood from the subglacial caldera lake. The earthquake was recorded well by the Iceland Hotspot Project seismic experiment.

Iceland has a heterogeneous crust, with variable thickness, and thus a 1D structural model is not ideal for waveform modeling. We investigated the earthquake with a point-source full moment-tensor (FMT) inversion method using regional long-period seismic waveforms and a composite structural model of Iceland based on modeling of teleseismic receiver functions and surface-wave dispersion. When such a model is used, the waveform modeling yields a NDC solution with a strong, vertically oriented compensated linear vector dipole component and a statistically insignificant volumetric contraction. The absence of a volumetric component is surprising and cannot be explained by shear slip on a planar fault. A possible mechanism that can produce an earthquake without a volumetric component involves two offset sources with similar but opposite volume changes. We show that although such a model cannot be ruled out, it is unlikely. We simulated different caldera geometries and rupture scenarios on the walls of a conical surface in order to compare the obtained moment tensor solutions with the observed moment tensor when the point-source approximation is used. These experiments support a super-shear rupture extending unilaterally accross one-half perimeter of the caldera as a likely scenario.

If studied in different frequency bands, the point source MT inversion fails to simultaneously explain the observed data, and this indicates the presence of finite-source effects. Using a 3D model of the Icelandic crust and upper mantle, we perform a probabilistic finite source inversion. One of the most robust outcomes of this is a well-constrained source duration with approximately equal amount of energy radiated by individual segments. This indicates that the caldera dropped coherently as a single block. We speculate that the earthquake accompanied a small-scale eruption that went unnoticed prior to the caldera drop caused the earthquake. The caldera drop could have increased the pressure in the magma chamber thus inducing the principal eruption.

2. Background

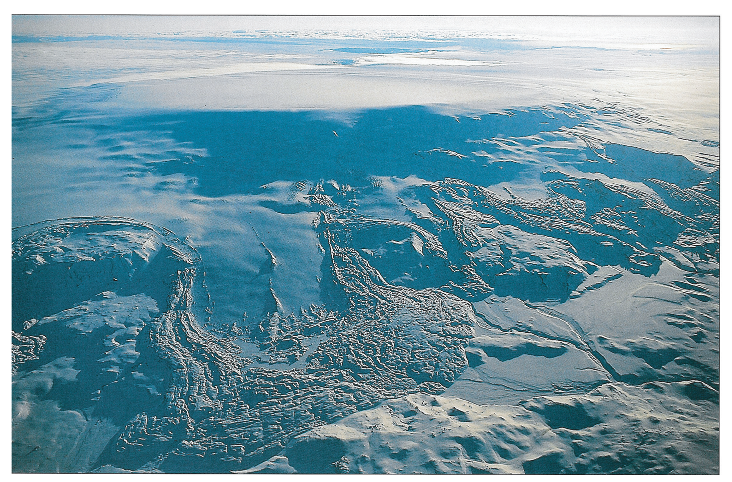

A remarkable series of seismic and magmatic events beneath the Vatnajökull icecap in Iceland occurred in 1996, and ultimately led to a breakout flood (jökulhlaup) from the Grimsvötn volcano subglacial caldera lake. A sequence of earthquakes commenced September 29, starting with a magnitude 5.6 earthquake in the Bárdarbunga volcano (left). Similar earthquakes had occurred in this area previously. Ten earthquakes clustered around the Bárdarbunga caldera are reported in the Global Centroid Moment Tensor catalog for the period 1976-1996 (*Nettles and Ekström, 1998*). However this time the event was followed by a swarm of small earthquakes that migrated toward a neighboring volcano, Grímsvötn, and culminated in a subglacial volcanic eruption (below; an airplane is seen above the eruption).

The main event, a Mw=5.6 earthquake, displayed an unusual pattern of seismic radiation, suggesting a non-double-couple (non-DC) mechanism. Studies of the event using teleseismic long-period and intermediate period surface wave data (*Nettles and Ekström, 1998*) and regional Icelandic data, based on a simple one-dimensional wave-speed model (*Konstantinou et al., 2003*) gave solutions with large compensated linear vector dipole (CLVD) components with approximately vertically oriented tensional major dipoles. *Nettles and Ekström (1998)* proposed that the derived non-double-couple (NDC) source mechanisms result from slip on an outward-dipping cone-shaped ring fault beneath the caldera, as a result of a change in pressure in the volcano's shallow magma chamber. *Konstantinou et al. (2003)* also reported an (8.5%) implosive isotropic component, and concluded that it was statistically significant.

Photo taken by Oddur Sigurdsson, Iceland Geological Survey

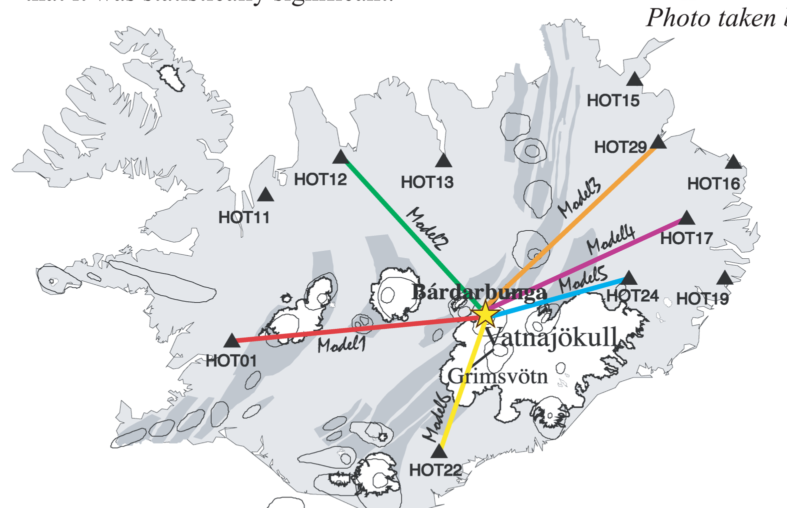

MODEL 5

Z_1 (km)	Z_2 (km)	V_P (km/s)	V_S (km/s)	ρ (g/cm^3)
0.0	0.5	2.932	1.666	1.708
0.5	1.0	4.263	2.422	2.134
1.0	2.0	4.537	2.578	2.222
2.0	3.0	4.724	2.684	2.282
3.0	4.0	4.851	2.756	2.322
4.0	5.0	5.275	2.997	2.458
5.0	6.0	5.798	3.295	2.625
6.0	10.0	6.096	3.463	2.721
10.0	24.5	6.686	3.799	2.910
24.5	29.5	7.051	4.006	3.026
29.5	39.5	7.488	4.254	3.166
39.5	42.0	7.819	4.443	3.272
42.0	300.0	7.898	4.488	3.297

A useful dataset with which to study the event was collected by the regional-scale Iceland Hotspot seismic experiment (*Foulger et al., 2001*). Studies using these data have resolved many details of the complex crustal structure of Iceland. We decompose moment tensor as described in section 2.6 of *Julian et al. (1998)* and used, for example, in *Dreger et al. (2000)*. The most difficult task was determining structural Green's functions. We generated Green's functions for crustal models determined by simultaneously inverting teleseismic receiver functions and surface-wave dispersion curves (e.g. *Du and Foulger, 2001*). Using a single model for Iceland to compute Green's functions for all source-receiver paths did not yield good fits to the observed waveforms, especially when waveforms from more than two stations were analyzed. We obtained significantly better results when we used the composite wave-speed model. An example of one segment (Model 5) of such composite model is shown on the left.

3. Full moment tensor complete-waveform (point-source) inversion, observations and sensitivity tests

Restrained (DC+CLVD)

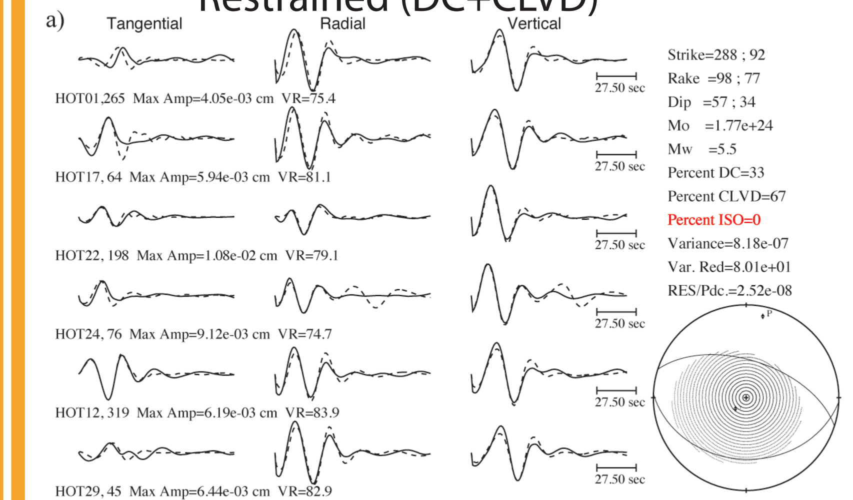

Unrestrained (DC+CLVD+ISO)

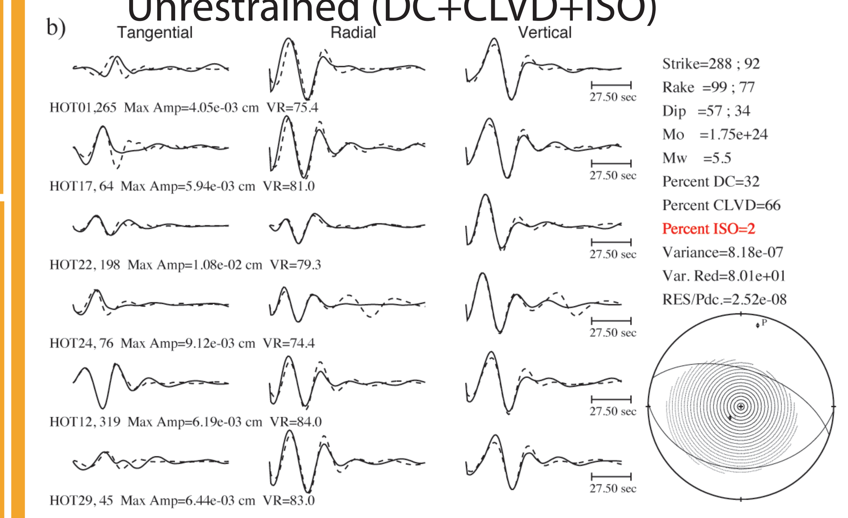

Jack-knife sensitivity test

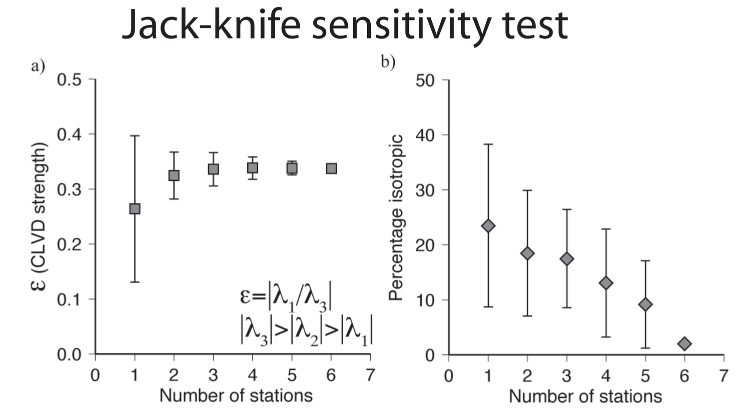

Different set of stations

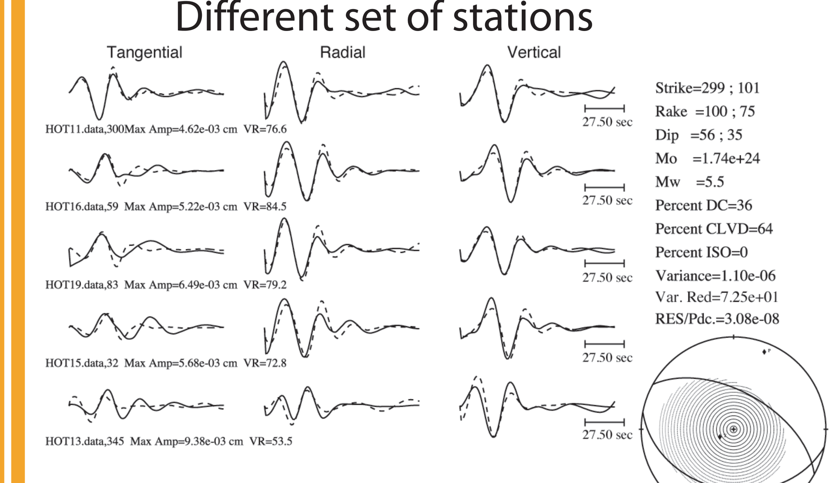

Inadequate number of stations

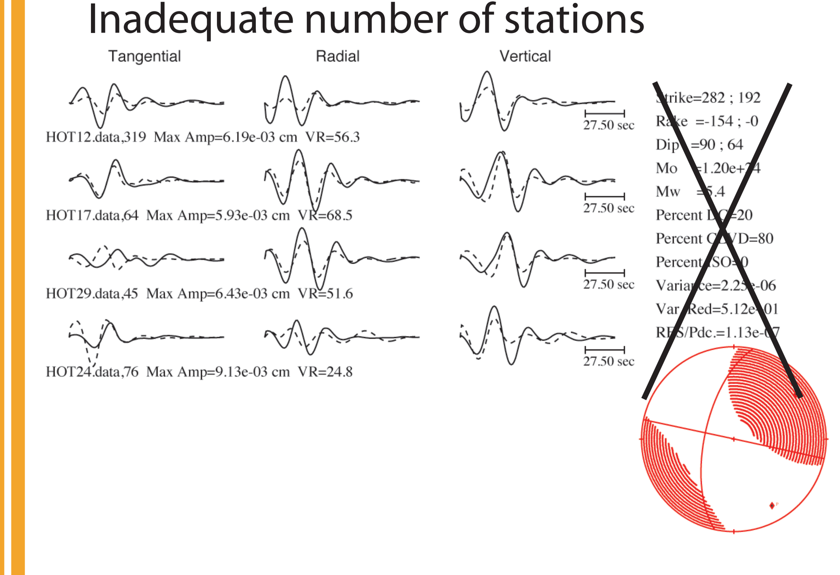

The deviatoric inversion of data from stations with good azimuthal coverage and using the composite model defined in the previous section yielded a NDC solution with a 67% CLVD component (Figure a) on the left), while the full moment tensor (FMT) resulted in a similar, 66% CLVD component, accompanied by an insignificant volumetric contraction (ISO=2%; Figure b) on the left). We performed a jack-knife test where we examined the stability of the size of the CLVD and ISO components as a function of the number of stations used in the inversion. We found that six was the optimal number of stations to resolve any possible ISO component. Inversions using data from other groups of stations revealed that the result is stable and well constrained. One such configuration of stations and corresponding best fits are shown in Figure entitled "Different combination of stations". We also present a case where a wrong solution is obtained by using inadequate number of stations (Figure in the lower left corner).

Two compensating sources

Since the mechanism for the main event appears to be strongly NDC without a large ISO component, we speculate that a net zero volumetric component is possible if the inflation moment equals the deflation moment in a mass-exchange process carried by a fluid flow, causing cancellation. We considered a system of two magma chambers (a) and a magma chamber and a vertical, horizontally opening crack (b).

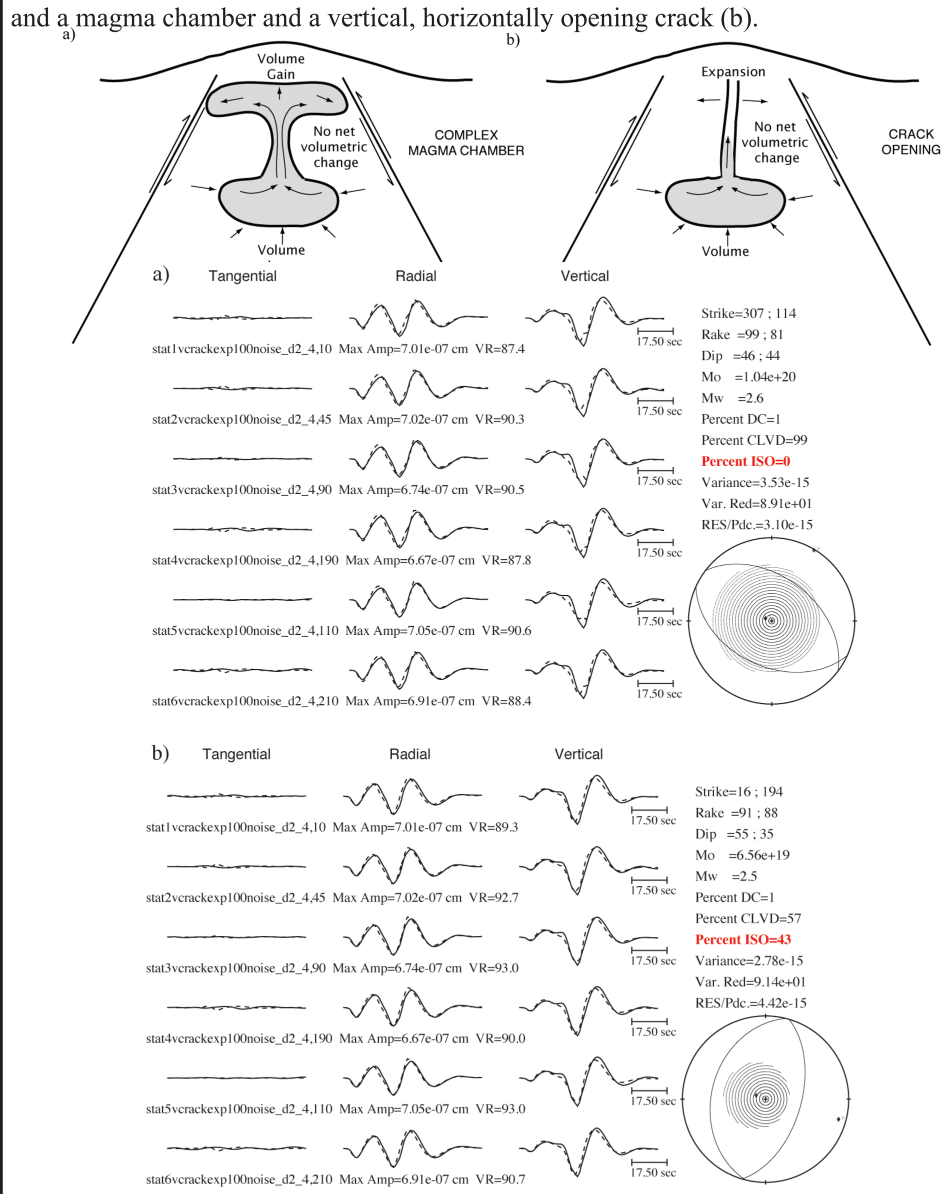

Figure above shows examples of the deviatoric (a) and full moment tensor (b) inversion results for two mutually compensating sources - an explosion at 4 km depth and a horizontal, vertically opening crack at 2 km depth. The waveforms corresponding to this configuration of sources are shown by solid lines. Synthetic waveforms are 1D Green's functions, based on slightly imperfect wave-speed models (shown by dashed lines) and a depth of 3 km. As Figure (b) shows, significant improvement in waveform fits and large, yet false isotropic component is retrieved from the inversion. This is opposite from what was observed for the Bárdarbunga, 1996 earthquake.

Rupture extent and fault orientation sampling

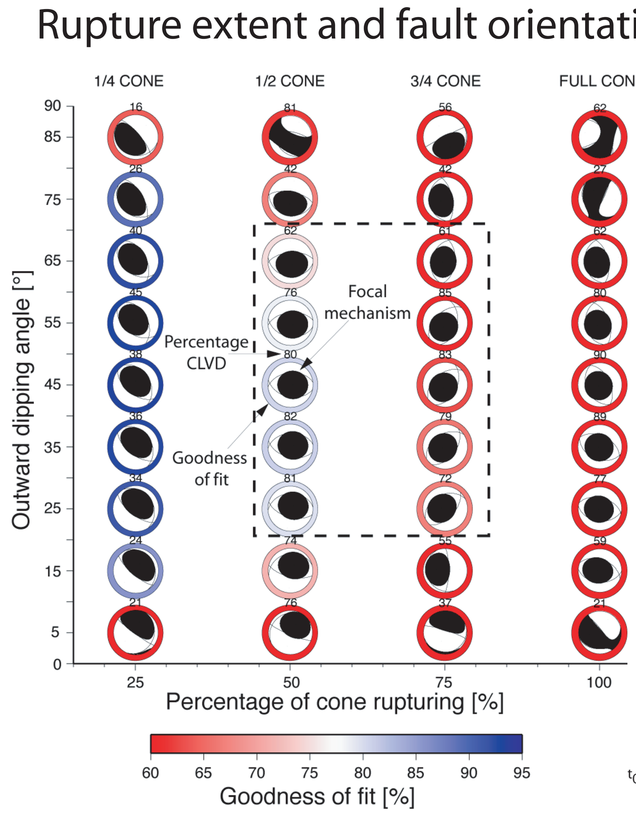

The area confined within a dash rectangle indicates the point source MT solutions that are similar to the solution for the mainshock (in terms of the waveform fits, focal mechanisms and percentage of CLVD.

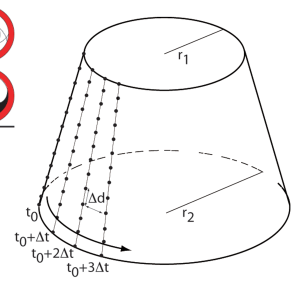

How well point-source approximation describes moment tensor of real sources?

In order to answer this important question, we designed a series of experiments in which we simulated finite source processes on a rupture surface shaped as a cone, designed so that its dimensions were similar to those of the caldera. We used the e3d finite differences method (Larsen and Shultz, 1995) and a large number of sources distributed in time and space to produce finite source synthetic "data" before performing a point-source inversion. Some of the scenarios are shown on the figures below. Based on the obtained moment tensors, we can make qualitative conclusions about likely cone inclination and extent (Figure in the lower center) of the rupture surface. Only half-cone unilateral, or full cone super-shear bilateral ruptures match the observation for the Bardarbunga mainshock.

Instantaneous drop (unphysical case)

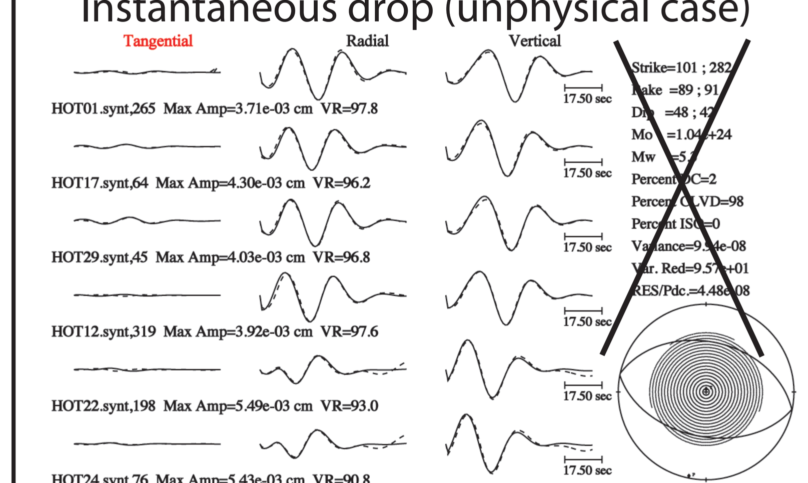

1/4 cone unilateral rupture

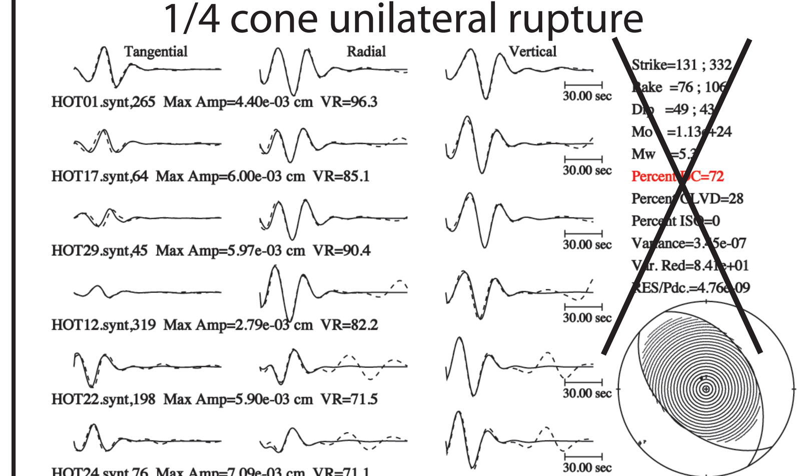

Full cone unilateral rupture

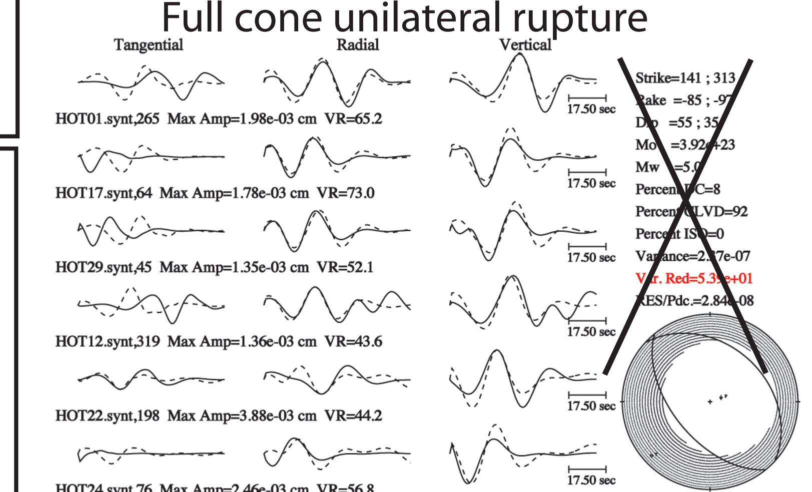

Full cone super shear bilateral rupture

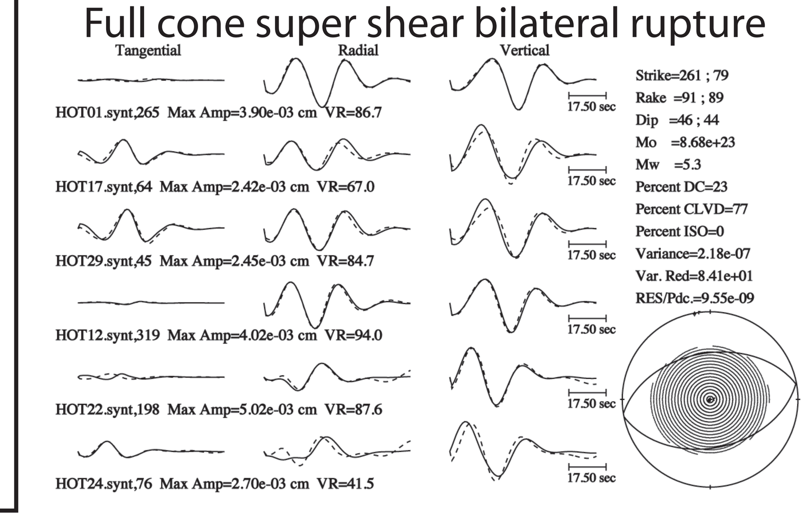

4. Kinematic Finite-Source Inversion

Verification of the structural model of Iceland and finite source effects

We constructed a 3D model that is based on a spline interpolation of vertical velocity profiles that were derived from simultaneous inversion of receiver functions and surface wave dispersion data (e.g. *Du and Foulger, 2001*). Crustal thickness of our model (vertical exaggerated) is shown below.

We first performed a point-source moment tensor inversion for an aftershock that occured on October 1, 1996 in three frequency bands centred around 0.1 Hz, 0.15 Hz and 0.2 Hz, using a spectral-element approach by *Fichtner and Igel (2008)*. With several exceptions, the waveforms in all three frequency bands are well recovered. This indicates that the structural model is accurate at frequencies below and including 0.2 Hz. The central figure below shows the comparison of the observed vertical component waveforms (solid lines) and synthetics (dashed lines) for the 0.2 Hz data.

When the same is repeated for the mainshock, we observe the discrepancies between the point-source synthetics and data, which we attibute to finite source effects. Figure at the bottom shows the comparison between data and synthetics for 0.2 Hz. Note that the observed moment tensor solution (with 71% CLVD) is similar to that of the previous studies using long period regional waveforms (*Nettles and Ekström, 1996; Tkalčić et al., 2009*).

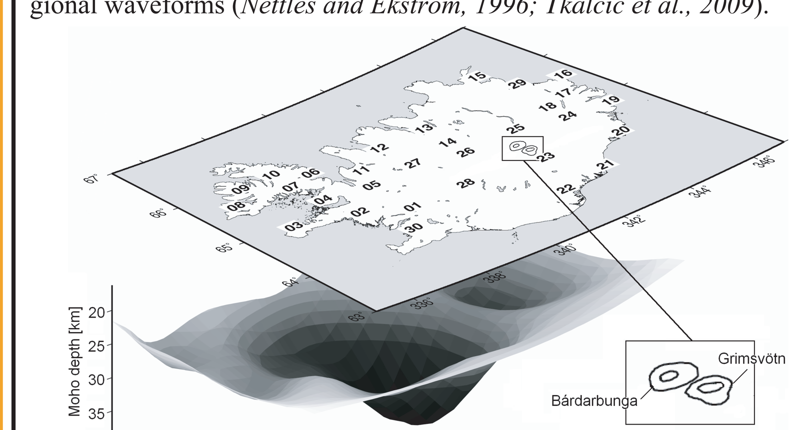

M_L=3.3 Aftershock (5s)

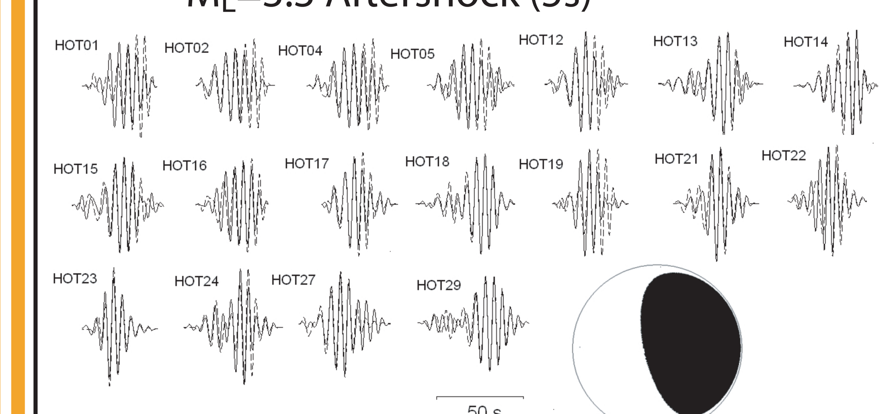

M_W=5.6 Mainshock (5s)

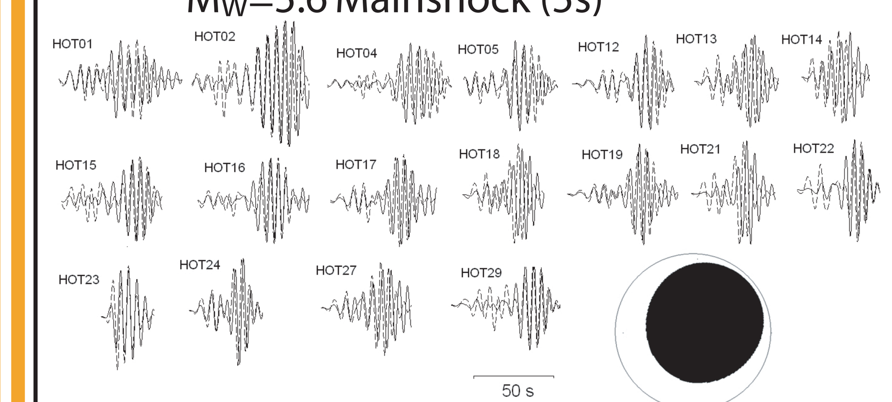

Probabilistic finite-source inversion

We subdivided the ring fault in 10 regularly spaced subfaults extending to 2 km depth, although we acknowledge that the vertical extend of the rupture is poorely constrained. We invert for the subfault moment magnitudes. We also allowed for a discrete inclination of the fault segments (0º, -15º and +15º). The rupture process on each subfault is characterized by a local rupture time and a downward local displacement.

We compute marginal probability density functions (PDF) via a Monte Carlo integration that is based on 10 million randomly generated fault models. The marginal probability densities for the rupture time and magnitudes are shown in the figures below in the form of histograms, where the height of each bar indicates the probability that a given parameter falls into the interval covered by the width of that bar. Gray bars indicate the most probable model. Also shown are probability distributions as gray scale images in circular form.

The PDFs for the rupture time indicate that the rupture is likely to have initiated in the north-western part of the ring fault. The rupture spread around the ring fault in possibly less than 3 seconds. The PDFs for the relative magnitudes show little variation, which indicates that each subfault radiated approximately the same abount of seismic energy.

Rupture time

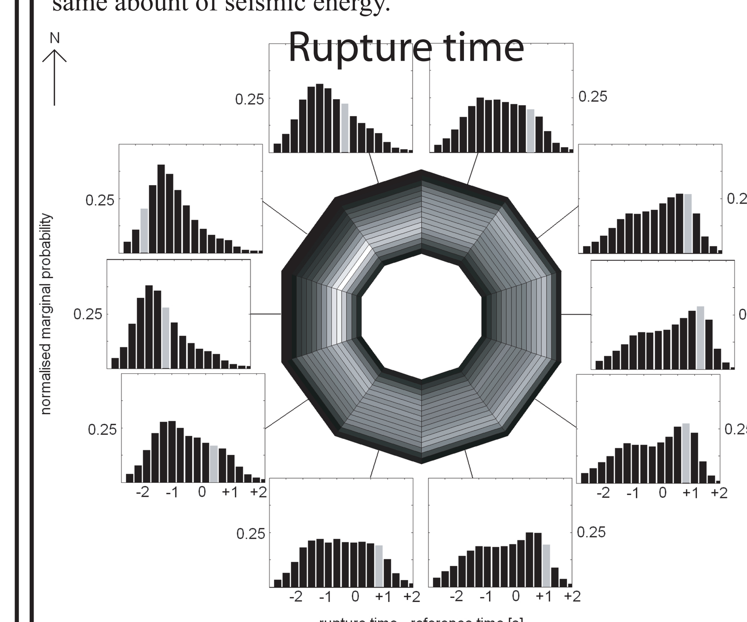

Magnitudes

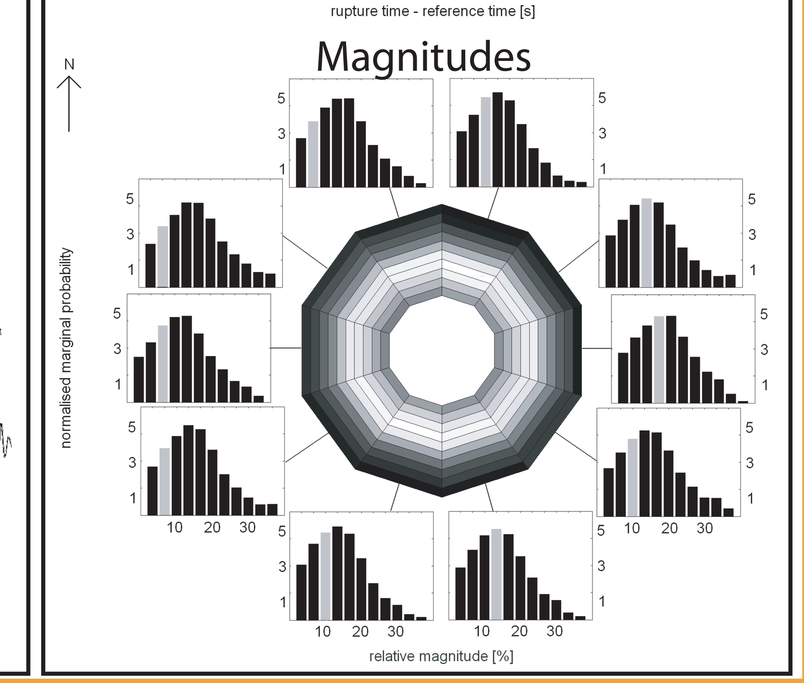

5. Conclusions and references

The FMT solution using a composite structural model of Iceland and a point-source approximation shows a 66% CLVD, 32% DC and a statistically insignificant 2% volumetric (isotropic) contraction. The lack of net volumetric component is surprising. We have shown that a possible volcanic mechanism that produces such an earthquake and involves two offset sources with similar but opposite volume changes is possible but an unlikely scenario to explain the observed radiation.

We have shown through the finite-source inversion that seismic data from a dense network can be used to constrain the kinematics of a volcanic caldera drop. Based on the equal amounts of energy radiated by the subfaults, we hypothesise that the caldera dropped uniformly after the rupture spread with a super-shear speed. We also hypothesise that a smaller subglacial eruption that triggered the caldera collapse occurred and went unnoticed. The major eruption after the earthquake is consistent with the classical model where the ring fault is located above the magma chamber.

Dreger, D.S., H. Tkalčić, and M. Johnston (2000), Dilational processes accompanying earthquakes in the Long Valley caldera, Science, 288, 122-125.

Du, Z. J., and G. R. Foulger (2001), Variation in the crustal structure across central Iceland, Geophys. J. Int., 145, 246-264.

Fichtner, A. and H. Igel (2008), Efficient numerical surface wave propagation through the optimization of discrete crustal models - a technique based on non-linear dispersion curve matching (DCM), Geophys. J. Int., 173(2), 519-533.

Fichtner, A. and H. Tkalčić (2009), Insights into the kinematics of a volcanic caldera drop: Probabilisitc finite-source inversion of the 1996 Bardarbunga, Iceland, earthquake, Earth Planet. Sci. Lett., submitted.

Foulger, G. R., M. J. Pritchard, B. R. Julian, et al. (2001), Seismic tomography shows that upwelling beneath Iceland is confined to the upper mantle, Geophys. J. Int., 146, 504-530.

Julian, B. R., A. D. Miller, and G. R. Foulger (1998), Non-double-couple earthquakes: 1. Theory, Rev. Geophys., 36, 525-550.

Konstantinou, I. K., H. Kao, C.-H. Lin, and W.-T. Liang (2003), Analysis of broad-band regional waveforms of the 1996 September 29 earthquake at Bárdarbunga volcano, central Iceland: investigation of the magma injection hypothesis, Geophys. J. Int., 154, 134-145.

Larsen, S. C., and C. A. Schultz (1995), ELAS3D: 2D/3D elastic finite-difference wave propagation code, Technical Report No. UCRL-MA-121792, 19 pp.

Nettles, M., and G. Ekström (1998), Faulting mechanism of anomalous earthquakes near Bárdarbunga volcano, Iceland, J. Geophys. Res., 103, 17 973-17 983.

Tkalčić H., D. S. Dreger, G. R. Foulger and B. R. Julian (2009), The puzzle of the Bardarbunga, Iceland earthquake: No volumetric component in the source mechanism, Bull. Seismol. Soc. Am., 99: 3077-3085.